

## Effect of Hazardous Bacteria Isolated From Copper Plumbing System on Microbiologically Influenced Corrosion of Copper

Carlos Galarce<sup>1,\*</sup>, Fabiola Pineda<sup>2</sup>, Diego A. Fischer<sup>1</sup>, Marcos Flores<sup>3</sup>, Ignacio T. Vargas<sup>1</sup>, Mamie Sancy<sup>4</sup> and Gonzalo E. Pizarro<sup>1,\*</sup>

<sup>1</sup> Departamento de Ingeniería Hidráulica y Ambiental, Escuela de Ingeniería, Pontificia Universidad Católica de Chile. Vicuña Mackenna 4860, Santiago, Chile.

<sup>2</sup> Departamento de Ingeniería Mecánica y Metalúrgica, Escuela de Ingeniería, Pontificia Universidad Católica de Chile. Vicuña Mackenna 4860, Santiago, Chile.

<sup>3</sup> Departamento de Física, Facultad de Ciencias Físicas y Matemáticas, Universidad de Chile. Beauchef 850, Santiago, Chile

<sup>4</sup> Escuela de Construcción Civil, Pontificia Universidad Católica de Chile. Vicuña Mackenna 4860, Santiago, Chile.

\*E-mail: [gpizarro@ing.puc.cl](mailto:gpizarro@ing.puc.cl)

Received: 6 November 2018 / Accepted: 31 December 2018 / Published: 7 February 2019

---

Plumbing systems can be affected by Microbiologically Induced Corrosion (MIC). Through this process, microorganisms can modify water quality and jeopardize consumers' health by releasing metal from pipes' surface into the water. While it is known that microorganisms' interactions increase their electrochemical effect on the metal surface, the effect of mixed communities and their interactions remain poorly understood. In this work, we investigated two hazardous bacteria isolated from a copper plumbing system, *Variovorax sp.*, and *Ralstonia pickettii*. Electrochemical impedance spectroscopy (EIS) showed a changing of oxide layer properties depending on immersion time. At short times, a capacitive behavior was observed at the low-frequency range, transiently including an additional inductive loop. At long times of exposure, the capacitive behavior disappears, and a Warburg behavior is present at the low-frequency. Interestingly, the corrosion was inhibited in pure culture tests, but this effect was reduced when the bacteria formed a consortium. In fact, EIS data show that the highest inhibitor activity was presented by *Variovorax sp.* pure culture, with 3.5-fold reduction in the corrosion rate compared with abiotic condition, and around of 2-fold when copper was exposed to *Ralstonia pickettii* and the consortium. XPS showed the formation of a different by-product of corrosion in the samples exposed to bacterial action. Moreover, SEM images revealed different bacterial growth behavior at the end of the test period. This research highlights the relevance of understanding the interactions of drinking water microbial communities

---

**Keywords:** Microbial corrosion; biofilm; copper; impedance; pathogen bacteria

## 1. INTRODUCTION

Microbiologically Induced Corrosion (MIC) or biocorrosion is the change in the corrosion process by the presence or activity of microorganisms [1]. This has a critical impact on drinking water systems thus affecting infrastructure and human health [2]. The complexity of the interplay between microorganisms, metal surface, and products of abiotic corrosion, and their different reaction kinetics, has prevented a clear understanding of the process.

Historically, copper has been used to build household plumbing systems due to its antiseptic properties [3, 4]. However, bacteria have been found living in copper plumbing systems [5–10]. Many of those are Gram-negative bacteria growing as a biofilm [9, 11–14]. This biological structure provides protection to various types of stresses such as disinfectants, pH, copper ions and temperature changes [15, 16]. One of the most important components of biofilm is the Extracellular Polymeric Substance (EPS), which helps to create a barrier that controls the diffusional process and chemical reactions with the environment. This barrier can favor the settlement of pathogenic bacteria, and thus, potential health hazards [9, 17]. This risk has led to an increase of the chlorine levels used to disinfect and reduce the bacterial load, reaching levels above the range suggested by WHO guidelines and adding yet another health concern [18].

The blue water phenomenon is the most extreme case of copper corrosion [19]. This occurs when high levels of copper are released into the water, giving a characteristic blue-green color [19, 20]. Unfortunately, little information and understanding are available about how bacteria influence this phenomenon.

This research presents with an opportunity to understand how biocorrosion occurs in a copper plumbing affected by blue water phenomenon. Here, two bacterial strains were isolated from such a system. One of them, *Variovorax sp*, has shown a high capacity to grow as a biofilm over copper pipes [10, 21], and it is able to tolerate high copper ( $127 \text{ mg} \cdot \text{l}^{-1}$ ) [21] and chlorine concentrations ( $16 \text{ mg} \cdot \text{l}^{-1}$  when growth like a biofilm) [18]. Moreover, a recent study reports the presence of transferable genetic elements, which could be involved in spreading antibiotic and disinfectant resistance genes to other bacteria nearby [22].

The second strain is *Ralstonia pickettii*, which is considered as an opportunistic pathogen [23, 24]. This species has been isolated from highly controlled clean environments such as hospitals [7, 25, 26] and ultrapure industrial water systems [25–27]. In water systems, *R. pickettii* strains often form biofilms, making them more resistant to biocides and complicating their eradication [27]. Moreover, it has been reported that *R. pickettii* has antibiotic resistance genes [28] which confer a wide resistance to many antimicrobial agents [25]. Furthermore, *R. pickettii* has shown a high resistance to copper concentrations (around 200 to  $600 \text{ mg} \cdot \text{l}^{-1}$ ) [29–31], allowing the bacterial growth in the copper plumbing system.

This study aims to understand how these two copper-tolerant bacteria modify the corrosion process in a copper plumbing system. Specifically, we will examine how bacterial interactions could affect the water quality by producing a higher release of corrosion by-products and/or pathogenic biofilm detachment.

Therefore, the electrochemical behavior of copper was evaluated through electrochemical impedance spectroscopy and surface analysis, when exposed to both, *Variovorax sp.*, and *Ralstonia pickettii*. The results allowed to estimate the effect on copper corrosion produced by each bacterium and when they interacted forming a microbial consortium.

## 2. MATERIALS AND METHODS

### 2.1. Isolation and Identification of Microorganisms

Copper pipe samples were taken from the suburbs of Olmué, Chile (33°00'S 71°12'O), a rural area that has shown severe copper corrosion in their plumbing system. *Bacteria* were isolated from the inner wall of one-year-old copper pipes, using lysogeny broth medium (Difco™). The individual strains of *Variovorax sp.* and *Ralstonia pickettii* and their consortium were cultured in a modified MSVP (Minerals Salts Vitamins Pyruvate) medium [32], with a concentration of pyruvate of  $4,4 \cdot 10^{-4}$  M to ensure a minimum source of organic matter. MSVP was selected because it has been shown to minimize the complexation of heavy metals [32].

Bacterial strain identification was done through partial sequencing of 16S rRNA and alignment with the BLAST GenBank [33]. 16S rRNA gene was amplified by PCR with the following settings: initial denaturation at 94°C for 5 min, followed by 30 cycles of denaturation at 94°C for 1 min, annealing at 55°C for 1 min, and extension at 72°C for 1 min. The last extension step was longer (10 min). An aliquot of the PCR product was electrophoresed in a 1.0 % agarose gel (Cleaver, Scientific Ltd) and stained with GelRed™ (Biotium). Afterward, the concentration of the PCR product was estimated by comparing with a standard (Low DNA Mass Ladder; Gibco BRL) [33]. The PCR product was sent to Macrogen Inc. for sequencing analysis.

### 2.3. Electrochemical Measurements

A typical three-electrode electrochemical cell was used. It consisted of a cylinder of PMMA (poly (methyl methacrylate)) fixed on the copper sample surface, providing a working electrode area of 31,17 cm<sup>2</sup>. A calomel electrode and platinum grid used as reference and counter electrode, respectively. The surface of copper was polished with fine sandpaper (2400-grit waterproof) and then it was cleaned with distilled water and acetone [34]. Copper coupons were sterilized with alcohol, washed with distilled water and exposed to UV light for 15 min before performing the electrochemical test using a Biologic VSP device, operating at the corrosion potential.

Electrochemical impedance spectroscopy (EIS), was performed using a peak-to-peak sinusoidal potential perturbation of 10mV and a frequency range extended from 100 kHz to 3 mHz, with 8 points per decade. Three independent samples were analyzed for each time and conditions. The immersion time was 1, 5, 7, 14, 21, 28, 35 and 60 days. All measurements were obtained under static conditions.  $|Z|$  value was corrected as described by Tran *et al.* [35]. Results were analyzed through the fitting of a proposed equivalent circuit (EC) (Figure1) using Zview® software. EC core was previously reported by Webster

*et al.*,2000[36]. The quality of fitting to the equivalent circuit was judged by chi-square ( $\chi^2$ ) value. The capacitance elements in the electrical equivalent circuit were replaced by constant phase elements (CPE). The elements of the circuit are as follows:  $R_{\text{bulk}}$  is the solution resistance,  $R_{\text{ct}}$  is the charge-transfer resistance for copper dissolution,  $C_{\text{dl}}$  is the double-layer capacitance,  $W$  is a diffusion component representing diffusion of copper ions through the copper oxide film and/or biofilm,  $R_{\text{pore}}$  is the pore resistance,  $C_{\text{film}}$  is the oxide film/or biofilm capacitance,  $R_{\text{ox}}$  is the oxide resistance and  $C_{\text{ox}}$  is the oxide capacitance.

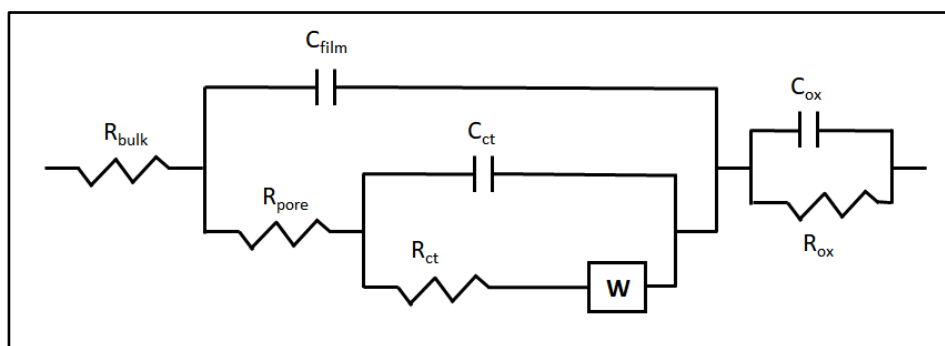


**Figure 1.** Equivalent circuit used to model to EIS data

#### 2.4. Oxide Thickness Calculations

The thickness of the oxide layer ( $\delta$ ) was determined using two approaches the Cole-Cole plot and the power law model formula [37–40] after exposure to both sterile and inoculated MSVP medium. The thickness of the oxide layer was obtained according to Equation 1, where the permittivity of vacuum ( $\epsilon_0$ ) was considered as  $8.8542 \times 10^{-14}$  F/cm, the dielectric constant of the oxide film was ( $\epsilon$ ), and  $C_\infty$  corresponds to the capacitance value obtained in the high frequency range of the Cole-Cole plot [39].

$$\text{Equation 1: } \delta = \frac{\epsilon \epsilon_0}{C_\infty}$$

Cole-Cole plots were obtained using the modulus of impedance corrected by ohmic-resistance ( $R_e$ ), as previously described [39]. In the present work,  $R_e$  was obtained as numerical graphical analysis. However, the amount of corrosion by-products and/or metabolic residues of bacterial consortium could have influenced the precision of the  $R_e$  value. This effect is better explained by Nguyen *et al.*[41], where small changes in the determination of  $R_e$  produce significant changes in the value of  $|Z|_{(f=5 \text{ mHz})}$ . However, the action of each isolated bacteria indicated that the  $|Z|_{(f=5 \text{ mHz})}$  values registered were higher than in other conditions (i.e., low corrosion was produced), but the thickness values estimated were lower. The values calculated were compared using power-law model (Figure S1).

#### 2.5. Scanning Electron Microscopy

The topography and structures formed on the samples' surfaces were analyzed by scanning electron microscopy (SEM) at the end of the experiment. The images were acquired by using an LEO 1420VP microscope (Cambridge, UK). According to the methodology described by Pavissich *et al.* [21],

coupons of 1.0 x 1.0 cm<sup>2</sup> were used for microscopic analyses. Coupons were fixed with 2.5 % (w/v) glutaraldehyde to avoid the detachment of bacteria from the surface. Samples were rinsed with sterile distilled water, postfixed with 1% (w/v) osmium tetroxide for 1 h and dehydrated in serial ethanol (50 – 100%) and acetone (100%) baths. Finally, after dehydration, coupons were dried to a critical point and coated with an ultrathin gold layer.

## 2.6. X-ray Photoelectron Spectroscopy

X-ray Photoelectron Spectroscopy (XPS) was used to determine the nature of the corrosion by-products formed on the copper surface. XPS spectra were recorded on an XPS-Auger PerkinElmer electron spectrometer Model PHI 1257, which included an ultra-high vacuum chamber, a hemispherical electron energy analyzer, and an X-ray source that provided unfiltered K radiation from its Al anode ( $h\nu = 1486.6$  eV). Pressure of the main spectrometer was in the range of  $10^{-6}$  Pa during data acquisition. The binding energy (BE) scale was calibrated using the peak of adventitious carbon, which was set to 284.8 eV [Handbook of XPS]. The samples were studied without preparation.

## 3. RESULTS AND DISCUSSION

### 3.1. Electrochemical measurements

#### 3.1.1. Open Circuit Potential (OCP)

Figure 2 shows the OCP responses for all systems as a function of exposure time. The results show how the OCP values moved closer to zero at all conditions, which can be explained by a decrease in the corrosion currents densities associated with the formation of an oxide layer. However, at the end of the experiment, the OCP values were only positive in inoculated media.

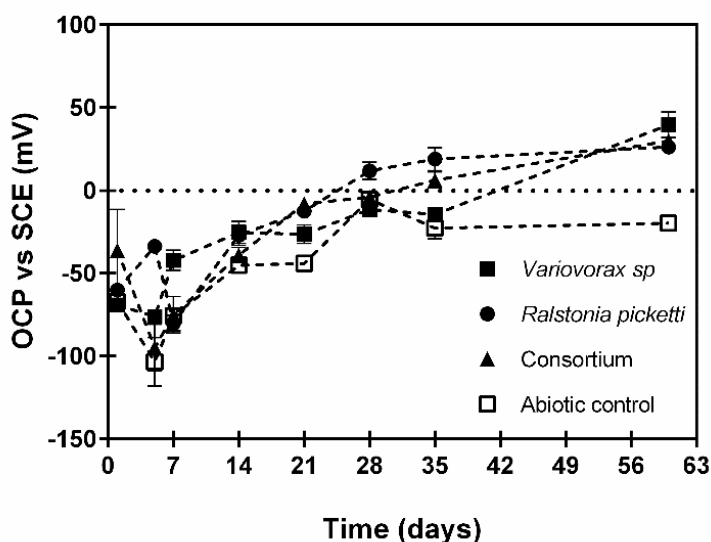


**Figure 2.** Open circuit potential of copper after exposure to MSVP inoculated with bacteria and abiotic control. Standard deviation bars are shown.

### 3.1.2. Impedance Results

The EIS results evidenced two different behaviors in function of exposure time. Figure 3 shows the Nyquist diagrams of copper after being exposed to MSVP in abiotic condition for 7 days. Nyquist diagrams revealed one capacitive loop at the range of high and medium frequencies, which can be associated with the formation of a porous film of  $\text{Cu}_2\text{O}$ . On the other hand, the inductive loop observed at low frequencies could be related to a relaxation process of adsorbed species due to the dissolution of copper [42].

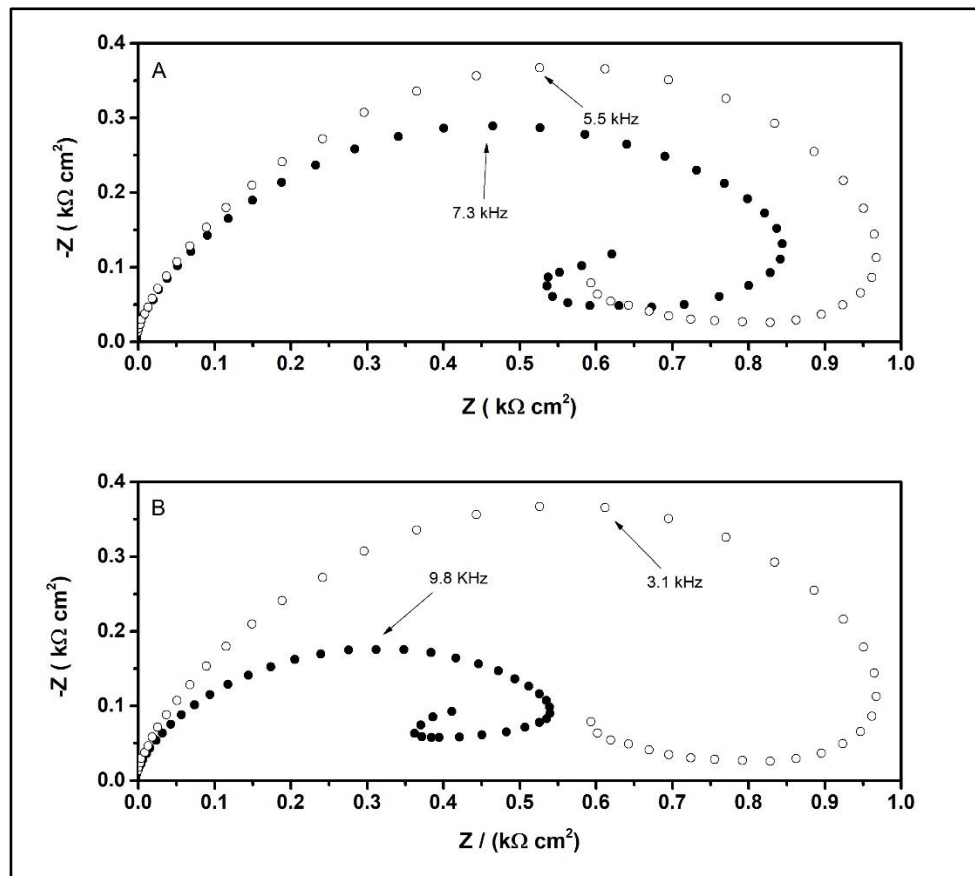


**Figure 3.** Nyquist diagrams of copper after exposure to MSVP inoculated with the bacterial consortium (A) and abiotic condition (B). Exposure time: 1 day (●) and 5 days (○).in abiotic condition.

After one week of exposure, EIS results revealed a different behavior in all conditions. At low frequencies, a Warburg behavior appeared (Figure 4). This is attributed to the oxygen-mass transport through the oxide film, similar to other metals [43–45].

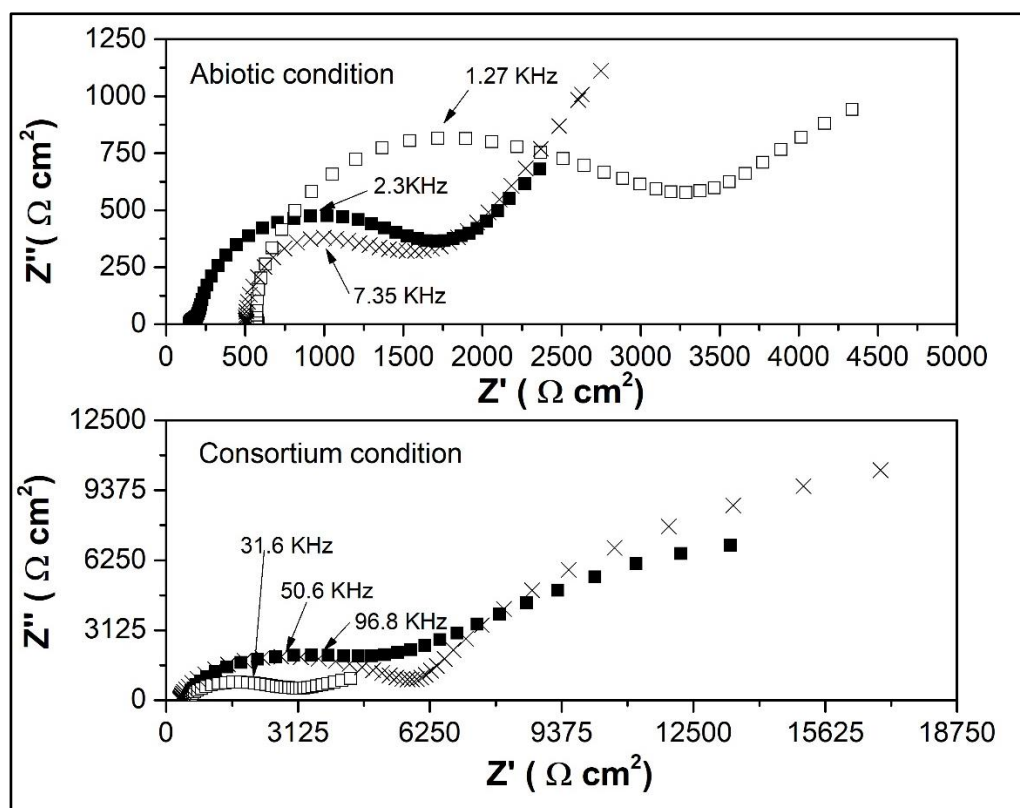


**Figure 4.** Nyquist diagrams of copper after exposure to abiotic conditions in MSVP as a function of exposure time. After 7 days (■), 21 days (□) and 35 days (×).

The impedance modulus at a low-frequency domain ( $|Z|_{(f=5 \text{ mHz})}$ ) was used as an approximation of the polarization resistance of the system for the analysis of impedance data. The values were greater than the abiotic control while the exposure time was longer, which might indicate a decrease in the corrosion rate, which is in accordance with the OCP results. Copper coupons exposed to *Variovorax sp.* and the bacterial consortium, showed a decrease in the  $|Z|_{(f=5 \text{ mHz})}$  values between days 7 and 28, from 270 to 130  $\Omega\text{cm}^2$  for *Variovorax sp.* and from 460 to 190  $\Omega\text{cm}^2$  for the consortium. (Figure 4). This behavior could be attributed to the oxide dissolution reaction. In contrast, *R. pickettii* kept stable values of around 200  $\Omega\text{cm}^2$ , between 7 to 28 days of exposure. The difference between OCP data and impedance results can be explained by the interference of microbial on electrochemical turnover reactions that occur over the metal surface. The abiotic condition also had stable values, around 75  $\Omega\text{cm}^2$ , until the 35 days of exposure (Figure 5).

After 60 days of exposure, the  $|Z|_{(f=5 \text{ mHz})}$  peak average was reached for all conditions (Figure 5). In the abiotic condition, the  $|Z|_{(f=5 \text{ mHz})}$  values were lower than all the inoculated samples, which suggests that the bacteria have an inhibitory effect on the copper corrosion. The comparison of  $|Z|_{(f=5 \text{ mHz})}$  suggests that *Variovorax sp.* pure culture was 1.8 times less corrosive than the consortium, and 3.5 times less corrosive than abiotic condition. On the other hand, *R. pickettii* was 11% less corrosive than the consortium, and 2.4-fold less corrosive than the abiotic condition. This indicates that the consortium is more corrosive than each bacterial pure culture. In summary, two aspects can be distinguished of electrochemical measurements. First, *Variovorax sp.* and *R. pickettii* reduce the copper corrosion under

the conditions used, which it is depending on exposure time after to compare with the abiotic condition, and second, bacterial behavior was different when microorganisms were put together to create a consortium.

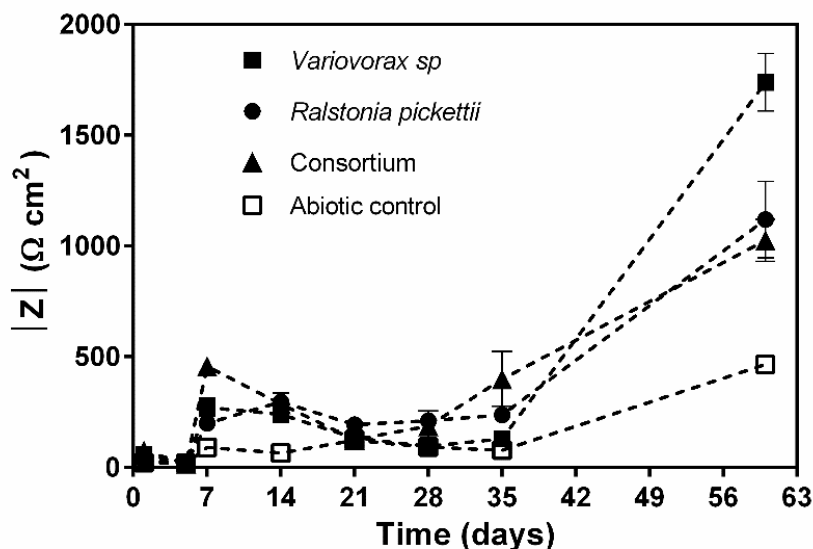


**Figure 5.** Average impedance modulus values of copper in MSVP medium as a function of exposure time. Standard deviation bars are showed.

EIS results can be mainly explained by the action of bacteria. Therefore, their mechanisms to offset the copper concentration are key to evaluate. For instance, *R. pickettii* possess a combination of adsorption and bioaccumulation capabilities, in conjunction with resistance mechanisms including influx and efflux pumps [31]. Nevertheless, the discharge of some bacterial exudate (e.g. catalase or organic acid) in the interface oxide/metal [46] cannot be ruled out, since it could also help in creating an environment that inhibits copper corrosion. However, its lower biofilm formation capacity on a copper surface resulted in it being less protected than *Variovorax sp.* On the contrary, *Variovorax sp.* can tolerate more copper due to its biofilm formation capacity. EPS could have affinity by cupric ions [47], which could reduce the concentration of free copper ions in the surrounding environment, allowing bacterial settlement. Therefore, the changes observed in the  $|Z|_{f=5 \text{ mHz}}$  values between 7 to 28 days may be related to bacterial attachment/detachment, suggesting that the difference in biofilm formation capacity could be an advantage to colonize the inner pipe. Notwithstanding, our data does not show discernible kinetics for bacterial detachment, so this hazardous phenomenon merit further study. All in all, the impedance results indicated that copper corrosion was strongly affected by the microorganisms, as results showed an increase of  $|Z|_{f=5 \text{ mHz}}$  values in comparison with the abiotic control (Figure 5).

The contribution of each component in the system was evaluated through a mathematical model. The data from Nyquist plots from day 7 to end time was fitted by using the equivalent circuit (EC) described in Figure 1. The results indicate that at the higher frequency relaxation, the  $n$  values were between 0.6 to 0.8, which are considered typical of the pure capacitive behavior of nonhomogeneous



surfaces [36]. No differences were observed in the resistance of oxide ( $R_{ox}$ ) and bulk ( $R_{bulk}$ ) among all conditions.

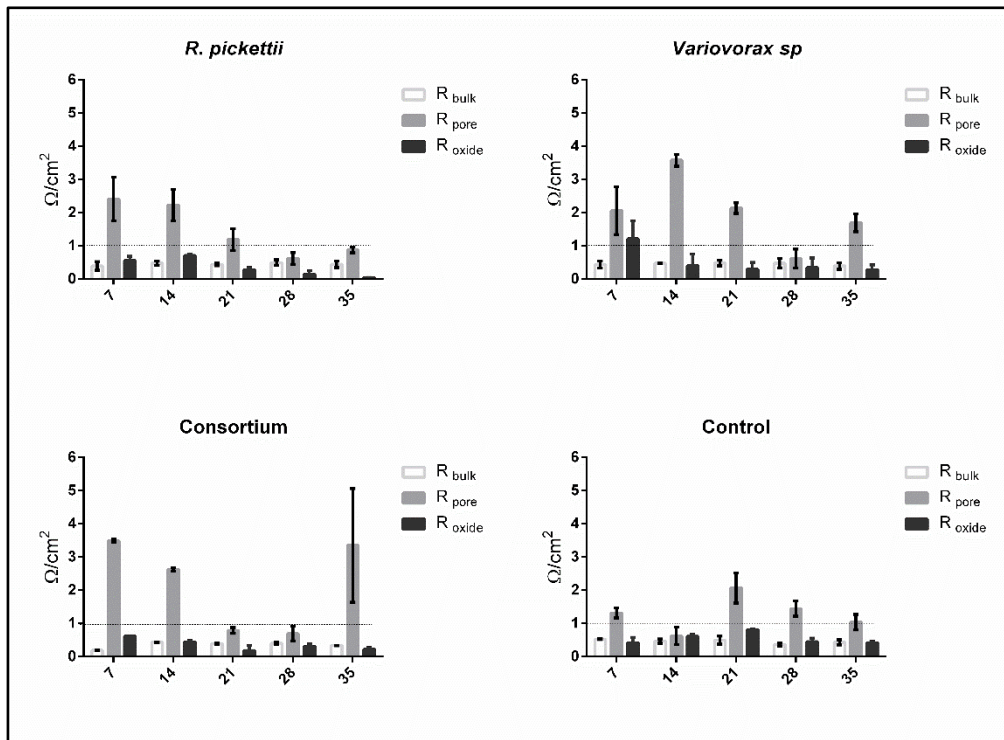


Figure 6. Average data values obtained for charge transfer resistances (R) until 35 days of exposure.

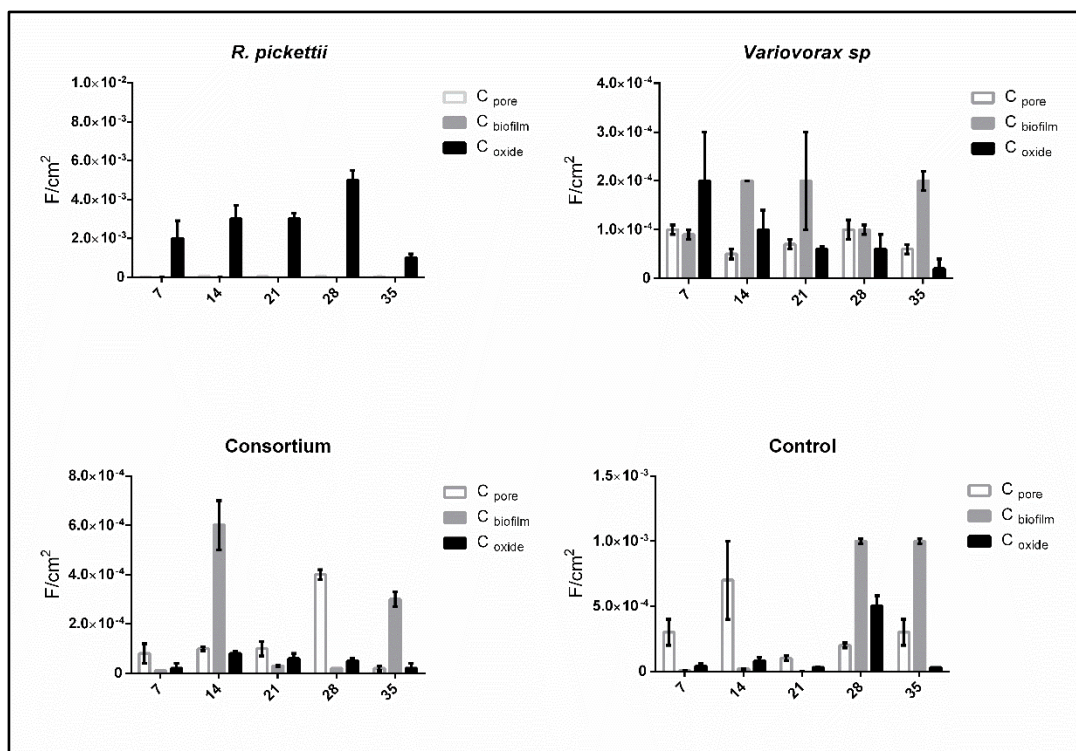
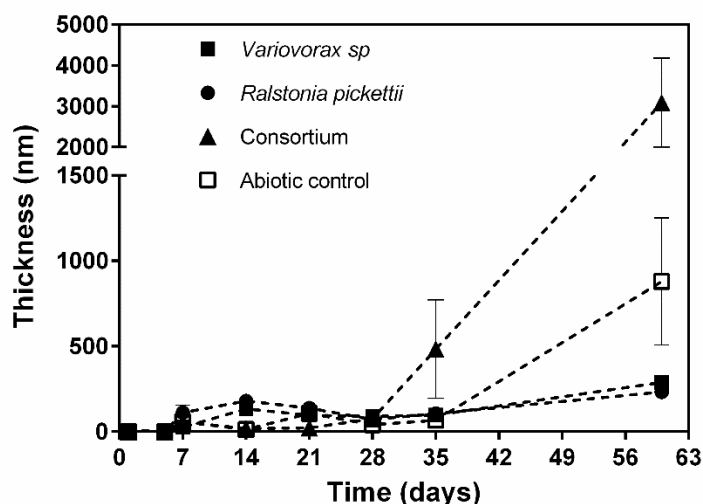


Figure 7. Average data values obtained for capacitances (CPE) until 35 days of exposure.

However, the distribution of resistance of pore ( $R_{\text{pore}}$ ) changed depending on the time and condition studied (Figure 6). The highest values of  $R_{\text{pore}}$  were observed in the inoculated samples. The analyses of capacitances in *R. pickettii* samples showed a high influence of oxide, where the  $C_{\text{ox}}$  until 2 order of magnitude values than  $C_{\text{film}}$  (average  $8 \times 10^{-6}$ ) and  $C_{\text{pore}}$  (average  $4 \times 10^{-5}$ ) (Figure 7). These large differences in CPE oxide values indicate that the oxide films behave very differently in terms of charge transfer resistance ( $R_{\text{oxide}}$ ), while the resistances across the conditions are similar. This suggests that the bacterial action on the surface changed the oxide layer properties.

The thickness of the oxide layer ( $\delta$ ) was determined through the study of a Cole-Cole plot to evaluate the influence of this variable. The  $\delta$  average values are shown in Figure 8. The results show each value obtained from Cole-Cole plot matched within the range calculated by the power-law model at each time and condition. Copper inoculated with the bacterial consortium showed the highest thickness values after 60 days of exposure. This method revealed the high variability of the oxide layer thickness on the copper coupons, especially in the case of the consortium after 60 days.



**Figure 8.** Variation of oxide layer thickness during the exposure time.

### 3.2. SEM Analysis

The surface of copper coupons after 60 days of exposure time in MSVP, in abiotic and biotic conditions, are shown in Figure 9. The abiotic condition shows a porous oxide layer, with surface cracks and ruts, together with some pitting on the surface (Figure 9.D). These conditions could promote the high reactivity of the surface, increasing the metal dissolution reaction. On the other hand, copper exposed to *Variovorax sp.* was covered by a biofilm (Figure 9.A). The picture also shows pitting and cracks over the surface. The irregular oxide layer of the surface suggests that copper released was the product of big detachments of copper oxide and bacteria.

A completely different picture was observed when copper was exposed to *R. pickettii*. The surface had deep grooves and cracks, but bacteria were nearly absent from the surface compared to the copper exposed to *Variovorax sp.* (Figure 9.B). Regarding copper exposed to the bacterial consortium,

the surface showed damage to the conditions observed in the samples exposed to *R. pickettii*, but no bacteria were observed on the surface (Figure 9.C).

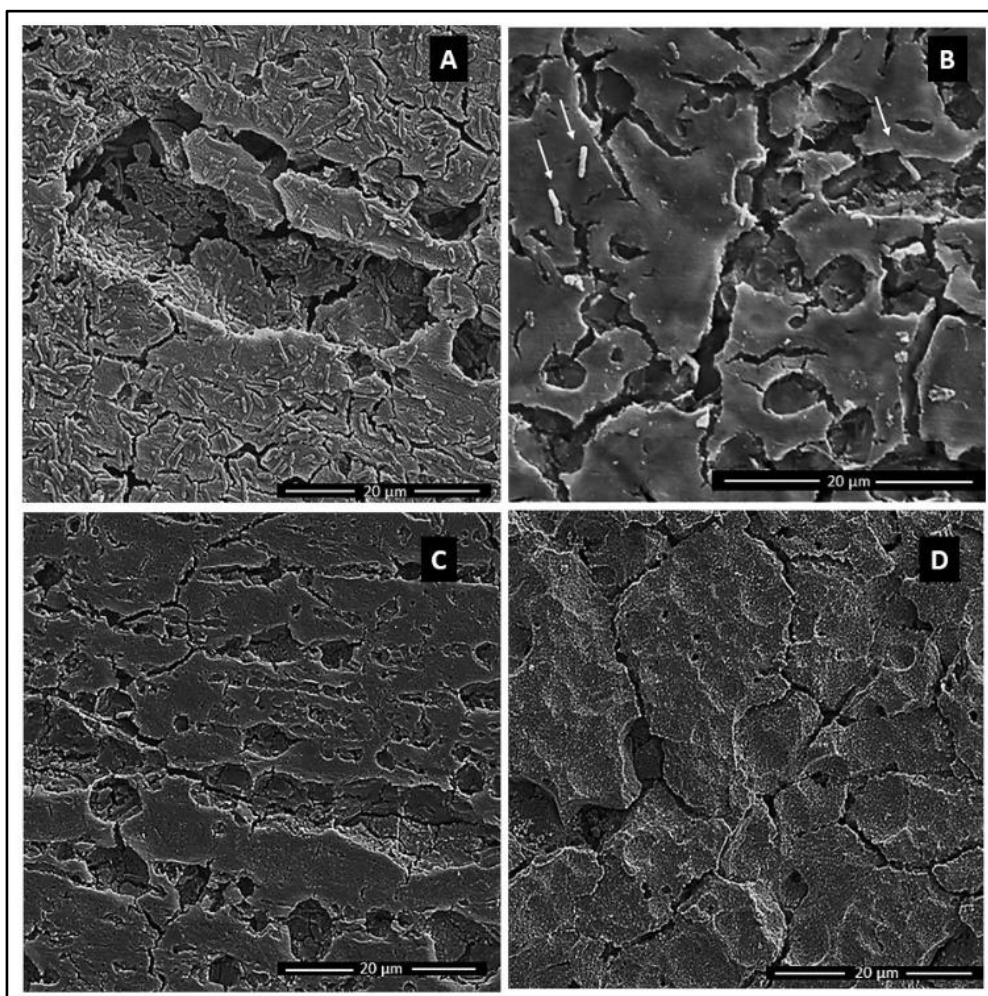


**Figure 9.** SEM images of copper coupons after 60 days of exposure time in MSVP. Copper inoculated with *Variovorax sp* (A), *Rasltonia pickettii* (B), Consortium (C), and Abiotic condition (D).

It is likely that the different EIS responses observed are caused by growing strategies of each bacteria, either as planktonic cells or as a biofilm. *Variovorax sp* showed a biofilm formation capacity on copper surface (Figure 9.A), which was also observed in previous studies [10, 21]. On the contrary, *R. pickettii* did not show a good biofilm formation capacity over the surface at the end of the exposure time (Figure 9.B). In fact, it only a few bacteria were found when an extensive inspection was done. This suggests that *R. pickettii* prefers to grow in the planktonic form in the study conditions. In previous reports, *R. pickettii* has been identified on biofilms in plastic water piping [26], however, this was not observed on copper. Copper toxicity did not appear to affect this, as bacteria in the samples were alive when tested with a live/dead assay [48] (data not shown) This is consistent with reports of *R. pickettii* living in high dissolved copper conditions [29, 30].

SEM images revealed no presence of bacteria on the copper surface exposed to the bacterial consortium. This suggests that the structure and the life cycle of biofilm is different when composed of two or more bacteria [49]. Inhibition of bacterial development due to the interaction between them has been reported [50–52]. This may be caused by a quorum sensing signal among the bacteria that conform the microbial community, which can grow as planktonic cells or as biofilm [9, 53, 54].

The observed biofilm's detachment could be a hazardous condition when these two bacteria interact on a plumbing system, as they could increase the bacterial load of drinking water, *R. pickettii* may have acted as an activator of biofilm replacement, so we only observed the results of the biofilm detachment with SEM images (Figure 9. C). Nevertheless, the predation between the bacteria cannot be excluded [49], since it was not possible to determine the consortium's species composition.

### 3.3. Surface Chemical Composition

Copper oxide layer composition developed over the metallic surface was obtained through the XPS technique after 60 days. XPS of the high resolution of copper revealed that the Cu2p signal had four components. The important ones were: Cu (0) +Cu(II) or Cu metallic + CuO at binding energy of 932.8 - 933.1 eV, Cu(I) or Cu<sub>2</sub>O at binding energy of 933.8 – 934.2 eV, and Cu(OH)<sub>2</sub> “hydroxylated copper” at binding energy of 935.1 – 935.8 eV. This last signal was only detected for samples with bacteria. A similar result was observed by a previous study using XAS [55]. The cuprite (Cu<sub>2</sub>O) was the predominant species in all conditions (Figure 10). No significant statistical differences among the samples exposed to bacteria were showed.

Cuprite (Cu<sub>2</sub>O) has been reported as a passivating agent in copper corrosion and it grows over time [56]. Furthermore, the literature suggests the cuprite film limits the diffusion of copper ions controlling copper corrosion [2]. However, this research indicate that biological activity was the main factor to affect copper corrosion, because of the similar percentages of cuprite found in all conditions by XPS analyses. Perhaps this amount of cuprite was not enough to protect copper from corrosion in the experimental conditions utilized. On the other hand, the percentage of copper hydroxide (Cu(OH)<sub>2</sub>) was higher in the copper exposed to bacteria. This could be another indication of the relevance of biological activity on copper corrosion since thermodynamics do not predict its presence in these conditions (pH=7). However, thermodynamic calculations based on bulk chemistry may not be accurate, since microbial activity can change the local chemical environment, inhibit oxide growth kinetics and decrease oxide film thickness [14]. Probably, bacteria change the electric potential or pH of their surrounding metal surface, which allows copper hydroxide production to be thermodynamically feasible as reported by Calle et al. [55]. Therefore, pH could have shifted to values near 8, a point where copper hydroxide can be generated as reported by *Obrecht et al* [57]. On the other hand, other studies that used EIS suggested that biofilms on copper create an acid microenvironment [2, 36]. However, each research is specific for each microorganism used. This situation indicate the needed to develop standardized tests for evaluate MIC [58].

The behavior of copper in abiotic conditions was in agreement with the results presented by *Ives et al* [59] where a non-defined porous oxide layer was formed (Figure 9.D). However, its thickness

determined using both the Cole-Cole and power-law model were less than in other studies [56, 60]. Medium components such as organic matter or orthophosphate could modify the protective character of the oxidation film on the copper surface [61, 62]. Despite the impact of the medium in accelerating corrosion, it is clear that bacteria have an inhibitory effect on the electrochemical behavior of copper. A corrosion-inhibitory effect has been reported for another bacteria [63], however, few reports have shown electrochemical results of bacterial interaction as it was done in this study. EIS results helped to understand how the biofilm acts as a diffusion barrier and produced experimental evidence of possible interactions between bacterial species in a biofilm, underscoring the need to further develop this research.

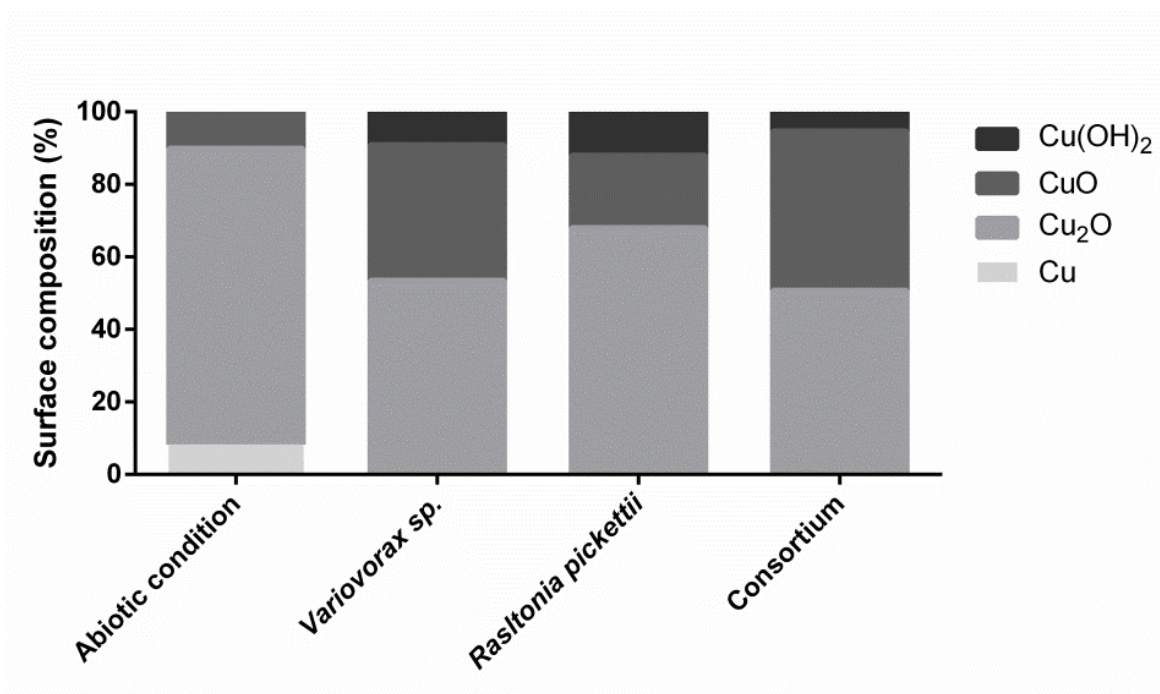


**Figure 10.** Surface composition of copper samples after 60 days of exposure.

#### 4. CONCLUSION

This study shows the effect of *Variovorax sp* and *Ralstonia pickettii* on copper corrosion. Both bacteria inhibit copper corrosion in the tested conditions, increasing the protective properties of cuprite layer due to the development of biofilm and other copper oxides on the surface during the exposure time. However, further studies are required to understand the interaction between these bacteria, as highlighted by the striking loss of *Variovorax sp*'s biofilm formation capacity when interacting with *Ralstonia pickettii*. This research provides evidence to support the potential danger of tap water microbial contamination due to biofilm detachment of bacterial consortiums.

## SUPPLEMENTARY MATERIAL

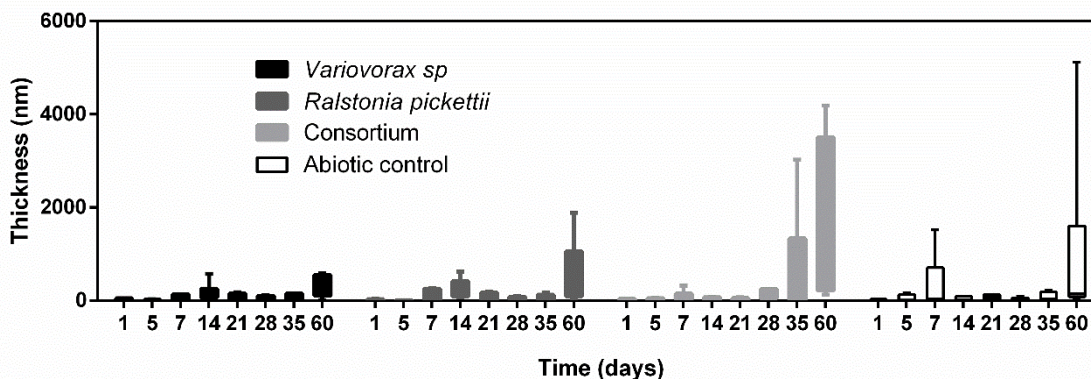


**Figure S1.** Range of thickness of oxide layer during exposure time using power-law model.

## ACKNOWLEDGEMENTS

Carlos Galarce acknowledges to CONICYT for his doctoral scholarships CONICYT-PCHA/Doctorado Nacional/2013- 21130365. Furthermore, the authors thank FONDECYT (Grant 1150357, 1160604, and 1181326), PIA-CONICYT (Grant ACT-1412). Special thanks to Nadine Pébère for all advice and methodological support in the determination of oxide layer thickness.

## References

1. "Standard Terminology Relating to Corrosion and Corrosion Testing ", ASTM International, ASTM G15-08, West Conshohocken, PA, 2010
2. I. Vargas, D. Fischer, M. Alsina, J. Pavissich, P. Pastén and G. Pizarro, *Materials*, 10 (2017) 1036
3. C. W. Keevil, *Water Sci. Technol.*, 49 (2004) 91
4. J. Luo, C. Hein, F. Mücklich and M. Solioz, *Biointerphases*, 12 (2017) 020301
5. I. Douterelo, M. Jackson, C. Solomon and J. Boxall, *Appl. Microbiol. Biotechnol.*, 100 (2016) 3301
6. J. Lu, H. Y. Buse, V. Gomez-Alvarez, I. Struewing, J. Santo Domingo and N. J. Ashbolt, *J. Appl. Microbiol.*, 117 (2014) 905
7. T. Coenye, J. Goris, P. De Vos, P. Vandamme and J. J. LiPuma, *Int. J. Syst. Evol. Microbiol.*, 53 (2003) 1075
8. M. J. Lehtola, I. T. Miettinen, M. M. Keinänen, T. K. Kekki, O. Laine, A. Hirvonen, T. Vartiainen and P. J. Martikainen, *Water Res.*, 38 (2004) 3769
9. S. Liu, C. Gunawan, N. Barraud, S. A. Rice, E. J. Harry and R. Amal, *Environ. Sci. Technol.*, 50 (2016) 8954
10. A. Reyes, M. V. Letelier, R. De la Iglesia, B. González and G. Lagos, *Int. Biodeterior. Biodegrad.*, 61 (2008) 135
11. D. J. Beale, R. Barratt, D. R. Marlow, M. S. Dunn, E. Palombo, P. D. Morrison and C. Key, *Biofouling*, 29 (2013) 283
12. W. Lin, Z. Yu, X. Chen, R. Liu, and H. Zhang, *Appl. Microbiol. Biotechnol.*, 97 (2013) 8393
13. D. A. Lytle and M. N. Nadagouda, *Corros. Sci.*, 52 (2010) 1927

14. I. T. Vargas, M. A. Alsina, J. P. Pavissich, G. A. Jeria, P. A. Pastén, M. Walczak and G. E. Pizarro, *Bioelectrochemistry*, 97 (2014) 15
15. T. E. Cloete, *Int. Biodeterior. Biodegradation*, 51 (2003) 277
16. C. Jungfer, F. Friedrich, J. Varela Villarreal, K. Brändle, H. Gross, U. Obst and T. Schwartz, *Biofouling*, 29 (2013) 891
17. Jost Wingender and Hans-Curt Flemming, *Int. J. Hyg. Environ. Health*, 214 (2011) 417
18. M. Schwering, J. Song, M. Louie, R. J. Turner and H. Ceri, *Biofouling J. Bioadhesion Biofilm J.*, 29 (2013) 917
19. M. Edwards, S. Jacobs and R. J. Taylor, *Journal-American Water Work. Assoc.*, 92 (2000) 72
20. M. M. Critchley, R. Pasetto and R. J. O'Halloran, *J. Appl. Microbiol.*, 97 (2004) 590
21. J. P. Pavissich, I. T. Vargas, B. González, P. A. Pastén and G. E. Pizarro, *J. Appl. Microbiol.*, 109 (2010) 771
22. S. Khan, C. W. Knapp and T. K. Beattie, *Environ. Process.*, 3 (2016) 541
23. C. R. Armbruster, T. S. Forster, R. M. Donlan, H. a O'Connell, A. M. Shams and M. M. Williams, *Biofouling*, 28 (2012) 1129
24. H. Sun, B. Shi, Y. Bai and D. Wang, *Sci. Total Environ.*, 472 (2014) 99
25. M. P. Ryan and C. C. Adley, *J. Med. Microbiol.*, 62 (2013) 1025
26. M. P. Ryan, J. T. Pembroke and C. C. Adley, *J. Appl. Microbiol.*, 103 (2007) 754
27. K. Mijndonckx, A. Provoost, C. M. Ott, K. Venkateswaran, J. Mahillon, N. Leys and R. van Houdt, *Microb. Ecol.*, 65 (2013) 347
28. S. Khan, C. W. Knapp and T. K. Beattie, *Environ. Process.*, 3 (2016) 541
29. K. T. Konstantinidis, N. Isaacs, J. Fett, S. Simpson, D. T. Long and T. L. Marsh, *Microb. Ecol.*, 45 (2003) 191
30. X. Xie, J. Fu, H. Wang and J. Liu, *African J. Biotechnol.*, 9 (2010) 4056
31. F. Yang, D. A. Pecina, S. D. Kelly, S. Kim, K. M. Kemner, D. T. Long and T. L. Marsh, *Environ. Technol.*, 31 (2010) 1045
32. G. M. Teitzel and M. R. Parsek, *Appl. Environ. Microbiol.*, 69 (2003) 2313
33. C. Alvarado G., M. Sancy, J. M. Blamey, C. Galarce, A. Monsalve, F. Pineda, N. Vejar and M. Páez, *Electrochim. Acta*, 247 (2017) 71
34. "Standard Practice for Preparing, Cleaning, and Evaluating Corrosion Test Specimens", ASTM International, ASTM G01-03, West Conshohocken, PA, 2017
35. T. T. M. Tran, B. Tribollet and E. M. M. Sutter, *Electrochim. Acta*, 216 (2016) 58
36. B. J. Webster, S. E. Werner, D. B. Wells and P. J. Bremer, *Corrosion*, 56 (2000) 942
37. C. H. Hsu and F. Mansfeld, *Corrosion*, 57 (2001) 747
38. B. Hirschorn, M. E. Orazem, B. Tribollet, V. Vivier, I. Frateur and M. Musiani, *Electrochim. Acta*, 55 (2009) 6218
39. T. Barrès, B. Tribollet, O. Stephan, H. Montigaud, M. Boinet and Y. Cohin, *Electrochim. Acta*, 227 (2017) 1
40. M. Benoit, C. Bataillon, B. Gwinner, F. Miserque, M. E. Orazem, C. M. Sánchez-sánchez, B. Tribollet and V. Vivier, *Electrochim. Acta*, 201 (2016) 340
41. A. S. Nguyen, N. Causse, M. Musiani, M. E. Orazem, N. Pébère, B. Tribollet and V. Vivier, *Prog. Org. Coatings*, 112 (2017) 93
42. M. Sánchez, N. Aouina, D. Rose, P. Rousseau, H. Takenouti and V. Vivier, *Electrochim. Acta*, 62 (2012) 276
43. M. Mirzaeian and P. J. Hall, *J. Power Sources*, 195 (2010) 6817
44. M. Stratmann and J. Müller, *Corros. Sci.*, 36 (1994) 327
45. Y. Wang, G. Cheng, W. Wu, Q. Qiao, Y. Li and X. Li, *Appl. Surf. Sci.*, 349 (2015) 746
46. S. Baeza, N. Vejar, M. Gulppi, M. Azocar, F. Melo, A. Monsalve, J. Pérez-Donoso, C. C. Vázquez, J. Pavez, J. H. Zagal, X. Zhou, G. E. Thompson and M. A. Páez, *Corros. Sci.*, 67(2013) 32

47. G. G. Geesey, L. Jang, J. G. Jolley, M. R. Hankins, T. Iwaoka and P. R. Griffiths, *Water Sci. Technol.*, 20 (1988) 161
48. P. L. Waines, R. Moate, A. J. Moody, M. Allen and G. Bradley, *Biofouling*, 27 (2011) 1161
49. H. C. Flemming, J. Wingender, U. Szewzyk, P. Steinberg, S. A. Rice and S. Kjelleberg, *Nat. Rev. Microbiol.*, 14 (2016) 563
50. H. A. Videla and L. K. Herrera, *Int. Microbiol.*, 8 (2005) 169
51. H. A. Videla and L. K. Herrera, *Int. Biodeterior. Biodegrad.*, 63 (2009) 896
52. P. J. Bremer and G. G. Geesey, *Appl. Environ. Microbiol.*, 57 (1991) 1956
53. B. Ramalingam, "The role of cell to cell interactions and quorum sensing in formation of biofilms in drinking water bacteria, in chemical and biological engineering", University of Sheffield, Sheffield, UK, (2012).
54. J. D. Shrouf and R. Nerenberg, *Environ. Sci. Technol.*, 46 (2012) 1995
55. G. R. Calle, I. T. Vargas, M. A. Alsina, P. A. Pastén and G. E. Pizarro, *Environ. Sci. Technol.*, 41 (2007) 7430
56. J. J. Shim and J. G. Kim, *Mater. Lett.*, 58 (2004) 2002
57. M. Obrecht and M. Pourbaix, *Am. Water Work. Assoc.*, 59 (1967) 977
58. S. A. Wade, M. A. Javed, E. A. Palombo, S. L. McArthur and P. R. Stoddart, *Int. Biodeterior. Biodegradation*, 121 (2017) 97
59. D. J. G. Ives and A. E. Rawson, *J. Electrochem. Soc.*, 109 (1962) 458
60. Y. Feng, W. K. Teo, K. S. Siow, K. L. Tan and A. K. Hsieh, *Corros. Sci.*, 38 (1996) 369
61. I. T. Vargas, M. A. Alsina, P. A. Pastén and G. E. Pizarro, *Corros. Sci.*, 51 (2009) 1030
62. S. Pehkonen, A. Palit and X. Zhang, *Corrosion*, 58 (2002) 156
63. N. Kip and J. A van Veen, *ISME J.*, 9 (2015) 542